Physical Mechanism of Ultrafast Flame Acceleration

Vitaly Bychkov,[1] Damir Valiev,[1,2] and Lars-Erik Eriksson[3]

[1]*Institute of Physics, Umeå University, SE-901 87, Umeå, Sweden*

[2]*Department of Materials Science and Engineering, Royal Institute of Technology, SE-10044 Stockholm, Sweden*

[3]*Department of Applied Mechanics, Chalmers University of Technology, 412 96 Gothenburg, Sweden*

(Received 30 April 2008; published 13 October 2008)

We explain the physical mechanism of ultrafast flame acceleration in obstructed channels used in modern experiments on detonation triggering. It is demonstrated that delayed burning between the obstacles creates a powerful jetflow, driving the acceleration. This mechanism is much stronger than the classical Shelkin scenario of flame acceleration due to nonslip at the channel walls. The mechanism under study is independent of the Reynolds number, with turbulence playing only a supplementary role. The flame front accelerates exponentially; the analytical formula for the growth rate is obtained. The theory is validated by extensive direct numerical simulations and comparison to previous experiments.

DOI: 10.1103/PhysRevLett.101.164501 PACS numbers: 47.70.Pq, 47.20.Ma, 47.27.Cn

A premixed combustion front propagates either as a slow subsonic flame (deflagration) or fast supersonic detonation [1]; their velocities differ by 3–4 orders of magnitude. However, a slow flame may spontaneously accelerate and trigger detonation [2–8]. A deflagration-to-detonation transition (DDT) remains one of the most intriguing and the least understood effects in hydrodynamics, combustion science, nonlinear physics, and astrophysics. The DDT produces detonation in the energetically cheapest way. It is the key point for explaining Thermonuclear Supernovae [9] and in many technological applications like design of pulse-detonation engines of next generation aircrafts [3]. It also stands behind many disasters like explosions in rockets and nuclear plants.

Spontaneous flame acceleration is the most important stage of the DDT. Flame acceleration in channels has been attributed qualitatively by Shelkin to wall friction and turbulence [2]. Turbulence was a fatal obstacle for quantitative understanding and predicting the DDT, since turbulence and turbulent burning is a field of modern physics, which is far from being fully understood yet despite a century of intensive research [1,10–12]. Recent theoretical advances and numerical simulations of the laminar DDT in smooth channels were a step forward in understanding the process [13–15], which demonstrated strong decrease of the acceleration rate with the increase of the Reynolds number. For this reason, thermal losses may stop flame acceleration in smooth channels. To achieve powerful flame acceleration, modern experiments use obstacles in the channels. Optimal obstacle design was actively debated at the last International Colloquium on Dynamics of Explosions and Reactive Systems (ICDERS-2007, Poitiers, France) [6–8]. Unfortunately, at present, obstacle design employs mostly a painful ''cut-and-try'' approach with minor theoretical understanding. It relies mostly on the qualitative Shelkin mechanism, with the general belief that the main role of the obstacles is only to create stronger turbulence.

Here, we show that the mechanism of ultrafast flame acceleration in obstructed channels has another physical nature, which is qualitatively different from the Shelkin explanation. We find that delayed burning between the obstacles creates a powerful jetflow driving the acceleration. The acceleration mechanism is independent of the Reynolds number, with turbulence playing only a supplementary role. The described mechanism is much closer in physical nature to initial acceleration of ''tulip'' flames explained by Clanet and Searby [16]. However, ''tulip'' flames accelerate only during a very short time, while the present mechanism works until detonation is triggered. We validate our theory by extensive numerical simulations and comparison to previous experiments.

Similar to modern experiments [3–7], we consider a channel of half-width R closed at one end, see Fig. 1. The channel is partly blocked by obstacles of height αR with free central part of half-width $(1-\alpha)R$. To elucidate the physical mechanism of flame acceleration, we start with tightly placed thin obstacles with spacing $\Delta z \ll \alpha R$. In this limit, turbulence may be neglected; laminar burning goes slowly in the pockets between the obstacles with normal velocity U_f. Burning matter expands by the factor $\Theta = \rho_f/\rho_b$ determined by the density ratio of the fresh and burnt gas; the expansion factor is typically $\Theta = 5$–8. Burnt gas flows out of the pockets with the speed $|u_x| = (\Theta - 1)U_f$. Coming into the free channel part, the flow changes direction to the axial one, accumulates into a strong jet and pushes the leading flame tip forward. Flame sweeps extremely fast along the free channel part leaving behind new pockets of the fresh fuel mixture. This produces a positive feedback between the flame and the flow and leads to strong exponential acceleration of the flame tip. At the beginning, the flame velocity is low, and the flow may be considered incompressible, $\nabla \cdot \mathbf{u} = 0$. Taking into account that $u_z = 0$ at the closed end $z = 0$, we find the velocity distribution in the free part of the channel with $|x| < (1-\alpha)R$

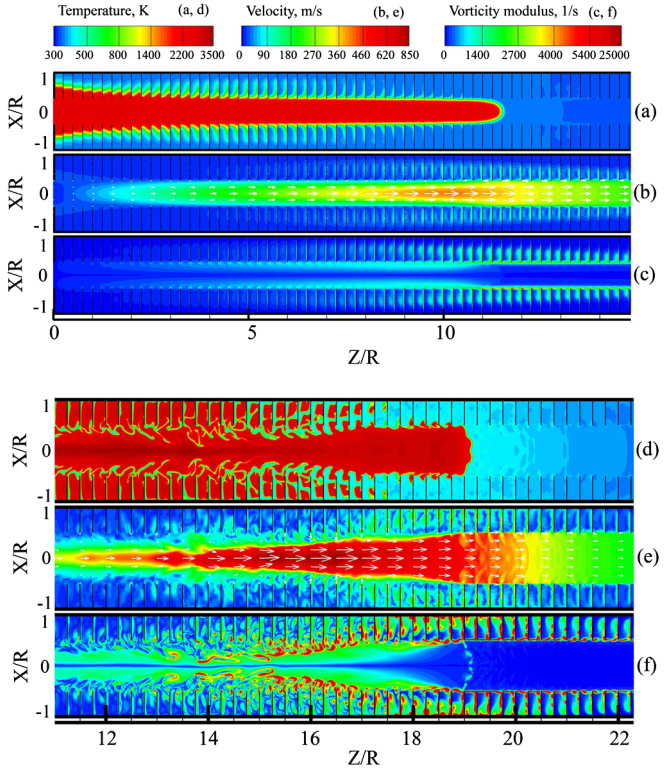

FIG. 1 (color online). Snapshots of temperature, velocity, and vorticity in the flow generated by an accelerating flame for $\Theta = 8$, $M = 0.001$, $\Delta z/R = 1/4$, $\alpha = 2/3$ (a)–(c) and $\alpha = 1/2$ (d)–(f).

$$(u_x; u_z) = \frac{(\Theta - 1)U_f}{(1 - \alpha)R}(-x; z). \quad (1)$$

The flow becomes quite strong at large distances from the tube end, $z/(1 - \alpha)R \gg 1$, when a large number of pockets contributes to the jet. The equation for the flame tip Z_f takes into account both the jetflow and intrinsic flame propagation with velocity ΘU_f with respect to the burnt matter

$$\frac{dZ_f}{dt} = u_z(Z_f) + \Theta U_f = \frac{(\Theta - 1)U_f}{(1 - \alpha)R}Z_f + \Theta U_f. \quad (2)$$

Solution to Eq. (2) describes powerful flame acceleration

$$\frac{Z_f}{(1 - \alpha)R} = \frac{\Theta}{\Theta - 1}[\exp(\sigma U_f t/R) - 1] \quad (3)$$

with the scaled acceleration rate $\sigma = (\Theta - 1)/(1 - \alpha)$ independent of the Reynolds number. This mechanism is much stronger than the classical Shelkin mechanism, which becomes extremely weak in smooth tubes at large values of the Reynolds number, see the quantitative theory [14,15]. On the contrary, the present mechanism works even in very wide obstructed tubes with ideally slip walls. Acceleration becomes stronger for larger thermal expansion Θ and larger blockage ratio α. Wall friction and turbulence play only supplementary roles in this mechanism, modifying burning between the obstacles. The described mechanism is much closer in physical nature to the initial acceleration of "tulip" flames explained by Clanet and Searby [16]; a more detailed theory of the process was developed recently in Ref. [17]. To see the similarity between these two mechanisms, let us consider flame ignition at the closed end $(x; z) = (0; 0)$ of the channel with obstacles. Reproducing calculations of Ref. [17] for the 2D channel, we obtain a finger-shaped flame front accelerating in the free part of the channel, $|x| < (1 - \alpha)R$, with the tip position described by Eq. (3). Still, a finger-shaped flame of Refs. [16,17] accelerates only during a very short time until it touches the sidewalls of the channel. The situation is different in channels with obstacles, where pockets with fresh fuel mixture separate the free part of the channel from the walls. Flame propagation in the pockets supports the jet in the free part of the channel and the exponential acceleration of the flame tip until detonation is triggered. Here, we can distinguish two phases of acceleration: a first phase where all the pockets of trapped mixture are still burning, and a second phase where initially ignited pockets successively burn out. In the second phase, the acceleration slows down, but only a little, by a factor marginally smaller than unity. During the interval between successive extinctions in pockets at the flame backside, many new pockets are ignited by the flame tip, and the flame keeps accelerating. Indeed, it takes time $\Delta t = \alpha R/U_f$ to burn all fuel mixture in a pocket between the obstacles. Then, backside of the flame front Z_b at time t coincides with the tip position at the time instant $t - \Delta t$, namely, $Z_b(t) = Z_f(t - \Delta t)$. Burning happens only in the domain $Z_b < z < Z_f$; only this domain contributes to the jet. Replacing Z_f by $Z_f(t) - Z_f(t - \Delta t)$ in the right-hand side of Eq. (2), we find the scaled acceleration rate from the equation $\sigma(1 - \alpha) = (\Theta - 1)[1 - \exp(-\sigma\alpha)]$. For typical parameter values $\alpha = 1/2$, $\Theta = 8$, we obtain reduction of the acceleration rate by 0.1% in comparison with Eq. (3). Formally, we may also look for a steady solution to modified Eq. (2), $Z_f = U_p t + Z_1$, where U_p is constant speed of the tip. However, solving Eq. (2), one finds $U_p = \Theta U_f[1 - \alpha(\Theta - 1)/(1 - \alpha)]^{-1} < 0$ for all realistic parameters of the problem $\Theta = 5$–8, $\alpha > 1/\Theta$. Negative flame speed does not have a physical meaning, while tiny plates with $\alpha < 1/\Theta$ cannot be treated as obstacles. Thus, exponential flame acceleration is the only physical solution to the problem. When a flame speed becomes comparable to the sound speed, c_s, gas compression tends to slow down the acceleration. Replacing $\nabla \cdot \mathbf{u} = 0$ by the complete equation $\nabla \cdot (\rho \mathbf{u}) = -\partial\rho/\partial t < 0$, we find gas compression reducing the jet velocity (1). In the case of small though finite compression, we can evaluate reduction of the jet velocity by the term $\int_0^{Z_f}(\rho^{-1}\partial\rho/\partial t)dz > 0$. This effect may be detected by simulations for high enough initial values of the Mach number.

We validated the analytical theory by direct numerical simulations of the two-dimensional Navier-Stokes equations for a compressible reactive flow. The simulations are performed in the same way as in our recent papers [14,15,17]. The homogeneous gas mixture obeys the ideal gas law $P = (1 - 1/\gamma)\rho C_P T$, where $C_P = 10^3\ \mathrm{m^2\,s^{-2}\,K^{-1}}$ is the specific heat at constant pressure and $\gamma = 1.4$ is the adiabatic index. Initial temperature and pressure are $T_f = 300$ K, $P_f = 10^5$ Pa. We used the free-slip and adiabatic boundary conditions at the walls and obstacle surfaces. The channel half-width was $R = 24L_f$, where $L_f = \mu_f/\mathrm{Pr}\,\rho_f U_f$ is the so-called flame thickness, $\mu_f = 1.7 \cdot 10^{-5}\ \mathrm{kg\,s^{-1}m^{-1}}$ is the viscosity coefficient of fuel mixture and the Prandtl number is $\mathrm{Pr} = 0.75$. We took the initial Mach number within the range of $\mathrm{M} = U_f/c_s = 10^{-3} - 10^{-2}$. The lower value of the Mach number $\mathrm{M} = 10^{-3}$ corresponds to realistic methane and propane flames. We model reaction rate by a single-step Arrhenius kinetics. The scaled activation energy was $E/R_pT_f = 32$, where R_p is the ideal gas constant. The reaction rate is assumed to be of the first order with respect to concentration of the fuel mixture and of the first or second order with respect to density. We took the Lewis number $\mathrm{Le} = 1$. We used the expansion factors $\Theta = 5$, 8, three values of the blockage ratio ($\alpha = 1/3$; 1/2; 2/3) and four values of spacing between the obstacles ($\Delta z/R = 1/4$; 1/2; 1; 2). The code is based on the cell-centered finite-volume method [18]. The numerical method has proved to be both accurate and robust for modeling of different kinds of complex reacting flows. The code has been validated by solving various hydrodynamic problems [18], and was utilized successfully in simulations of laminar flames at different conditions of burning [14,15,17].

Characteristic snapshots of the flame, the flow velocity, and the vorticity are shown in Fig. 1. Figures 1(a)–1(c) reproduce the theoretical limit in the best way with the realistically small initial Mach number and tightly placed obstacles. In agreement with the above theory, the strongly accelerating flame front is confined in the free part of the channel; burning in the pockets is delayed. The gas flow shows a strong jet in the free channel part with practically no turbulence. Figures 1(d)–1(f) show the flame front at the stage of developed acceleration, when the front propagation speed is comparable to the sound speed. Here, the central jet generates quite strong turbulence, which makes the flame shape corrugated with much faster turbulent burning in the pockets. Still, even in that case, we can distinguish the leading central part of the flame front and the strong jetflow. A corrugated turbulent shape of the flame front might conceal the physical mechanism of flame acceleration described above. Complications of turbulent burning were, probably, the main reason why this mechanism was not discovered previously. Still, this mechanism keeps working not only qualitatively, but quantitatively even for strongly corrugated turbulent flames. Figures 2 and 3 show the position of the flame tip versus time and the tip velocity versus its position. We can observe the simulation results with different parameters coming in groups (shown by different colors). We compare the scaled acceleration rates obtained in experiments [17], theory, and numerical simulations, denoted as σ_{exp}, σ_{th}, σ_{num}, respectively. Series of markers closest to the solid line in Fig. 2 correspond to the same simulation parameters as in Fig. 1 ($\mathrm{M} = 10^{-3}$, $\Theta = 8$). They reproduce the incompressible limit in the best way and show very good agreement with the theory, $\sigma_{\mathrm{num}} \approx 0.9\sigma_{\mathrm{th}}$; the deviation is comparable to the common accuracy of numerical simulations [14,15,17]. Large values of the Mach number are beyond our incompressible model. To explore the model limitations, we also performed simulations with large initial values of the Mach

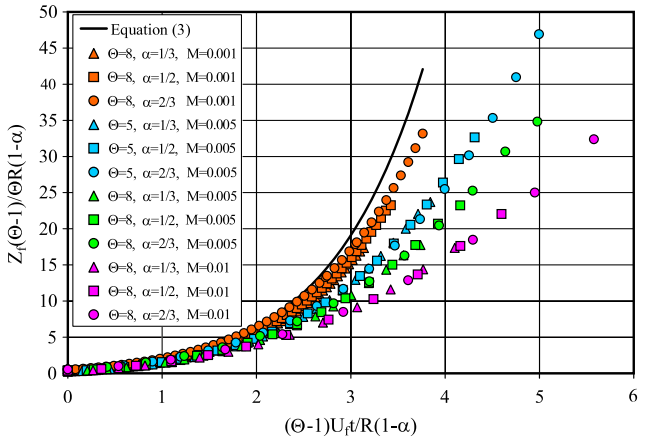

FIG. 2 (color online). Scaled position of the flame tip versus scaled time. Analytical solution (3) is shown by the solid line; numerical results are shown by markers. $\Theta = 5$, 8, $\mathrm{M} = 0.001$; 0.005; 0.01, $\alpha = 1/3$; 1/2; 2/3.

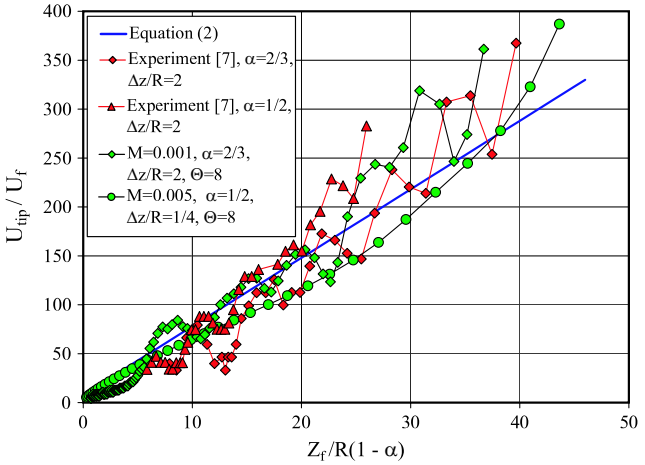

FIG. 3 (color online). Scaled velocity of the flame tip versus the scaled tip position. Solid straight line corresponds to the analytical solution (2), markers show experimental results of Ref. [7] and results of numerical modeling.

number. We observe noticeably slower exponential flame acceleration at larger values of the Mach number; the deviation between the theory and modeling happens as the local Mach number comes close to 1. The influence of gas compression on flame acceleration has not been investigated before; still, analyzing results of the previous works for smooth tubes [13–15], we come to the same conclusion as in the present Letter.

On the developed stage of flame acceleration, turbulence makes burning in the pockets faster and compensates for the influence of gas compression. As a result, the above theory describes quite well even the acceleration of a strongly turbulent flame. Figure 3 compares the theory and simulations to the experiments by Johansen and Ciccarelli [7], which are of the most recent and elaborated ones with the experimental setup geometry in line with the present theory and modeling. The experiments have been performed for a stoichiometric methane-air mixture. The flame speed in the methane-air mixture was measured in Ref. [19]; we also take into account corrections due to lower initial pressure of experiments [7]. Johansen and Ciccarelli [7] used obstacles with rather large spacing, which led to strong pulsations of the flame velocity. Our theoretical model is laminar, and it does not reproduce pulsations. Still, on average, the experiments, theory, and modeling are in a good agreement. We calculate the average acceleration rate using the linear dependence $U_{\rm tip}/U_f = \sigma_{\rm exp} Z_{\rm tip}/R + \Theta$, and find $\sigma_{\rm exp}/\sigma_{\rm th} \approx 0.98$; 1.1; 1.2 for the blockage ratios $\alpha = 2/3; 1/2; 1/3$, respectively. Similar to the experiments, we performed several simulation runs with large spacing between the obstacles $\Delta z/R = 1; 2$. Large spacing made the flame less confined, but it also led to stronger turbulence with pulsations of the flame velocity similar to the experiments [7]. Still, changing the spacing of the obstacles, we obtained only minor changes in the average flame speed with the above theory working quite well. In the simulations of Fig. 3 (circles), we also see an early stage of the explosion ahead of the accelerating flame. The explosion may be traced by rapid increase of the flame velocity at $Z_f/R(1-\alpha) = 35$–45. The explosion and detonation triggering is the final stage of DDT, which was also observed in the simulations and which will be presented in detail elsewhere. Thus, the present theory and modeling explain the physical mechanism of ultrafast flame acceleration observed in modern experiments on detonation triggering. Understanding of this physical mechanism gives the capability for better control of the flame acceleration and DDT timing in different applications, e.g., in pulse-detonation engines.

We thank Gaby Ciccarelli and Craig Johansen for the experimental data of Ref. [7]. The work was supported by the Swedish Research Foundation and by the Kempe Foundation.

[1] L. D. Landau and E. M. Lifshitz, *Fluid Mechanics* (Pergamon Press, Oxford, 1989).
[2] K. Shelkin, J. Exp. Theor. Phys. **10**, 823 (1940).
[3] G. D. Roy, S. M. Frolov, A. A. Borisov, and D. W. Netzer, Prog. Energy Combust. Sci. **30**, 545 (2004).
[4] G. Ciccarelli, C. Fowler, and M. Bardon, Shock Waves **14**, 161 (2005).
[5] M. Kuznetsov, V. Alekseev, I. Matsukov, and S. Dorofeev, Shock Waves **14**, 205 (2005).
[6] S. Frolov, I. Semenov, P. Utkin, P. Komissarov, and V. Markov, *Proceedings of 21st ICDERS, paper 215* (Poitiers, France 2007).
[7] C. Johansen and G. Ciccarelli, *Proceedings of 21st ICDERS, paper 242* (Poitiers, France 2007).
[8] V. Gamezo, T. Ogawa, and E. Oran, *Proceedings of 21st ICDERS, paper 114* (Poitiers, France 2007).
[9] P. Mazzali, F. Ropke, S. Benetti, and W. Hillebrandt, Science **315**, 825 (2007).
[10] B. Hof, C. van Doorne, J. Westerweel, and F. Nieuwstadt, Phys. Rev. Lett. **95**, 214502 (2005).
[11] G. Searby, F. Sabathier, P. Clavin, and L. Boyer, Phys. Rev. Lett. **51**, 1450 (1983).
[12] A. R. Kerstein, W. T. Ashurst, and F. A. Williams, Phys. Rev. A **37**, 2728 (1988).
[13] L. Kagan and G. Sivashinsky, Combust. Flame **134**, 389 (2003).
[14] V. Bychkov, A. Petchenko, V. Akkerman, and L. E. Eriksson, Phys. Rev. E **72**, 046307 (2005).
[15] V. Akkerman, V. Bychkov, A. Petchenko, and L. E. Eriksson, Combust. Flame **145**, 206 (2006).
[16] C. Clanet and G. Searby, Combust. Flame **105**, 225 (1996).
[17] V. Bychkov, V. Akkerman, G. Fru, A. Petchenko, and L. E. Eriksson, Combust. Flame **150**, 263 (2007).
[18] C. Wollblad, L. Davidsson, and L. E. Eriksson, AIAA J. **44**, 2340 (2006).
[19] G. Searby and J. Quinard, Combust. Flame **82**, 298 (1990).